Moroccan Journal of Chemistry
ISSN: 2351-812X
http://revues.imist.ma/?journal=morjchem&page=login
Zouitini & al. / Mor. J. Chem. 6 N°3 (2018) 391-403

Corrosion Inhibition Behavior of Quinoxaline Derivative as a Green Corrosion Inhibitor for Mild Steel in Hydrochloric Acid: Electrochemical, Weight Loss and DFT Simulations Studies

A. Zouitini[1], Y. Kandri Rodi[1], H. Elmselem[3]*, F. Ouazzani Chahdi[1], H. Steli[4], C. Ad[5], Y. Ouzidan[1], E. M. Essassi[2], A. Chetouani[3.6] and B. Hammouti[3]

[1]Laboratory of Applied Organic Chemistry, Faculty of Science and Technology, University Sidi Mohammed Ben Abdallah, Fez, Morocco

[2]Laboratoire de Chimie Organique Hétérocyclique, URAC 21, Pôle de Compétences Pharmacochimie, Université Mohammed V, Faculté des Sciences, Av. Ibn Battouta, BP 1014 Rabat, Morocco.

[3]Laboratoire de chimie analytique appliquée, matériaux et environnement (LC2AME), Faculté des Sciences, B.P. 717, 60000 Oujda, Morocco.

[4]Laboratoire mécanique & énergétique, Faculté des Sciences, Université Mohammed Premier, Oujda, Maroc

[5]Laboratory of process engineering, Department Process Engineering, Laghouat University, P.O Box 37G, Route de Ghardaïa, 03000, Laghouat, Algeria.

[6]Laboratore Chimie physique Centre regional des Métiers de l'Education et de Formation de l'oriental, Morocco.

** Corresponding author:*
h.elmsellem@gmail.com
Received 24 March 2018,
Revised 14 May 2018,
Accepted 03 July 2018

Abstract

The effect of quinoxaline derivative (AY20) against the corrosion of mild steel (MS) in 1 M acidic chloride (HCl) solution was investigated by chemical (weight loss – WL) and electrochemical (Tafel polarization and Electrochemical impedance spectroscopy) techniques. From all the four methods, it is inferred that the percentage of inhibition efficiency increases with increasing the inhibitor concentration from 10^{-3}M to 10^{-6}M. The adsorption behavior of inhibitor obeyed through Langmuir isotherm model. EIS technique exhibits one capacitive loop indicating that, the corrosion reaction is controlled by charge transfer process. Tafel polarization studies revealed that the investigated inhibitor is mixed type and the mode of adsorption is chemical in nature. Theoretical quantum chemical calculations were performed to confirm the ability of (AY20) to adsorb onto mild steel surface. The results obtained from different techniques are in good agreement.

Keywords: Quinoxaline derivative; Corrosion inhibitor; Steel; efficiency; EIS; DFT.

1.Introduction

Corrosion is a fundamental process playing an important role in economics and safety, particularly for metals and alloys. Corrosion can also be defined as a chemical reaction taking place at the surface of metals, which can be converted into a organic compounds [1-3]. Mild steel has found wide applications in a broad spectrum of industries and machinery; despite its tendency to corrosion. Because of the aggressiveness of acid solutions, inhibitors are commonly used to reduce the corrosive attack on metallic materials. Organic compounds rich in heteroatoms such sulphur, nitrogen and oxygen generally exhibit the best protection among corrosion [4–8]. Inhibitors are used in these processes to control metal dissolution as well as acid consumption. The uses of inhibitors are one of the most practical methods to inhibit corrosion of metals in many environments, especially in acidic media [9]. The inhibitor adsorption mode was strictly dependent on the inhibitor structure [10]. Data in the literature show that most organic inhibitors adsorb on mild steel by displacing water molecules on the surface and forming a compact barrier film [11–12]. Adsorption of inhibitors may blocks either cathodic, anodic, or both reactions.In chemistry, nitrogen-containing heterocycles are indispensable structural units for medicinal activities. Among this class of heterocyclic compounds, quinoxalines form an important biologically active molecules as there are various antibiotics such as hinomycin and levomycin, and actinoleutin[13–14]. Quinoxaline derivativesexhibit various biological activities includingantidiabetic[15], antibacterial[16], anticancer[17], and antifungal[18] activities.

The synthesis of new organic molecules offers various molecular structures containing several heteroatoms and substituents. In continuation of the encouraging results obtained by different synthetic inhibitors, we investigate the corrosion of mild steel in 1 M HCl by 1,4-dibutyl-6-methylquinoxaline-2,3(1H,4H)-dione compound. Weight loss tests and electrochemical techniques (potentiodynamic polarization and impedance measurements) have been used to study the effect of addition of this compound on the corrosion of steel in hydrochloric acid solution (1 M HCl) .The adsorption isotherm of inhibitor on steel surface and the standard adsorption free energy (ΔG_{ads}) are obtained.

2. Experimental

2.1. Synthesis and materials

2-1.1 Materials

The steel used in this study is a mild steel with a chemical composition (in wt%) of 0.370 % C, 0.230 % Si, 0.680 % Mn, 0.016 % S, 0.077 % Cr, 0.011 % Ti, 0.059 % Ni, 0.009 % Co, 0.160 % Cu and the remainder iron (Fe).

2.1.2. Solutions

The aggressive solutions of 1.0 M HCl were prepared by dilution of analytical grade 37% HCl with distilled water. The solution tests are freshly prepared before each experiment. The range of concentration of 1,4-dibutyl-6-methylquinoxaline-2,3(1H,4H)-dione (AY20) was 10^{-6} M to 10^{-3} M. Triplicate experiences were made to ensure the reproducibility.

2.1.3. Chemical Compound

Synthesis of 6-methyl-1,4-dihydroquinoxaline-2,3-dione (3)

To a solution of 4-Methyl-o-phenylenediamine**1** (8 mmol) was added oxalic acid **2** (8 mmol) in 16 ml of hydrochloric acid (4M). The mixture was refluxed for 4 hours. The black precipitate obtained is washed several times with distilled water.

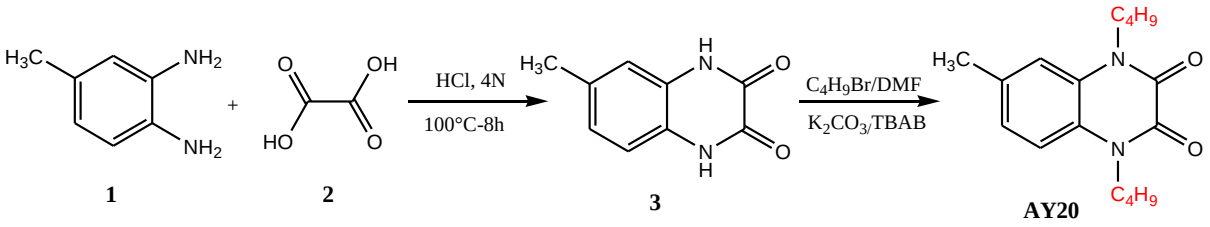

Synthesis of 6-methyl-1,4-dihydroquinoxaline-2,3-dione (3)

To a solution of 4-Methyl-o-phenylenediamine**1** (8 mmol) was added oxalic acid **2** (8 mmol) in 16 ml of hydrochloric acid (4M). The mixture was refluxed for 4 hours. The black precipitate obtained is washed several times with distilled water.

6-methyl-1,4-dihydroquinoxaline-2,3-dione (3)

Yield (90%) ; Mp : 361 °C ; ^{1}H NMR (DMSO-d_6) δ : 2,26 (s, 3H, C***H*****$_3$**) ; 6,87-7,28 (m, 3H, C***H*****$_{arom}$**) ; 11,83 (s, 2H, 2 N***H***) ; ^{13}C NMR (DMSO-d6) δ : 155,76 (***C***=O) ; 155,44 (***C***=O) ; 132,73 (***C***q) ; 125,92 (***C***q) ; 124,23 (***C***H$_{arom}$) ; 123,76 (***C***q) ; 115,61 (***C***H$_{arom}$) ; 115,44 (***C***H$_{arom}$) ; 21,01 (***C***H$_3$).

Synthesis of compound AY20.

To a solution of 6-methyl-1,4-dihydroquinoxaline-2,3-dione 0,3g (1,73 mmol) in DMF (20 ml), we have added 0.47g (3,61 mmol) of potassium carbonate and 0,1 mmol of tetra-n-butyl ammonium (BTBA), after 10 min of stirring 3,46 mmol of butylbromide were added, then the mixture was allowed to stir at room temperature for 12 hours.After filtration of salts, the DMF was evaporated under reduced pressure and the residue obtained is dissolved in dichloromethane, the organic phase was dried over Na_2SO_4 and then concentrated. The mixture obtained was chromatographed on Silica gel column (eluent : hexane/ethyl acetate (4/1)).

1,4-dibutyl-6-methyl-1,4-dihydroquinoxaline-2,3-dione (AY20)

Yield (89%) ;Mp : 118,3 °C ; ^{1}H NMR ($CDCl_3$) δ : 0,96-1,03 (m, 6H, 2C***H*****$_3$**) ; 1,44-1,55 (m, 4H, 2C***H*****$_2$**) ; 1,73 (m, 4H, 2C***H*****$_2$**) ; 2,44 (s, 3H, C***H*****$_3$**) ; 4,17-4,43 (m, 4H, 2C***H*****$_2$**) ;7,04-7,27 (m, 3H, C***H*****$_{arom}$**) ; ^{13}C NMR ($CDCl_3$) δ : 154,23 (***C***=O) ; 153,89 (***C***=O) ; 133,96 (***C***q) ; 126,59 (***C***q) ; 124,75 (***C***H$_{arom}$) ;124,44 (***C***q) ; 115,50 (***C***H$_{arom}$) ; 115 (***C***H$_{arom}$) ; 42,90 (***C***H$_2$) ;42,82 (***C***H$_2$) ; 28,90 (2***C***H$_2$) ; 21,24 (***C***H$_3$) ; 20,19 (2***C***H$_2$) ; 13,82 (2***C***H$_3$).

The analytical and spectroscopic data are conforming to structures of compound (**3a**) formed. 1H-NMR and 13C-NMR spectrums of compound (**AY20**) are showed below (Figure 1).

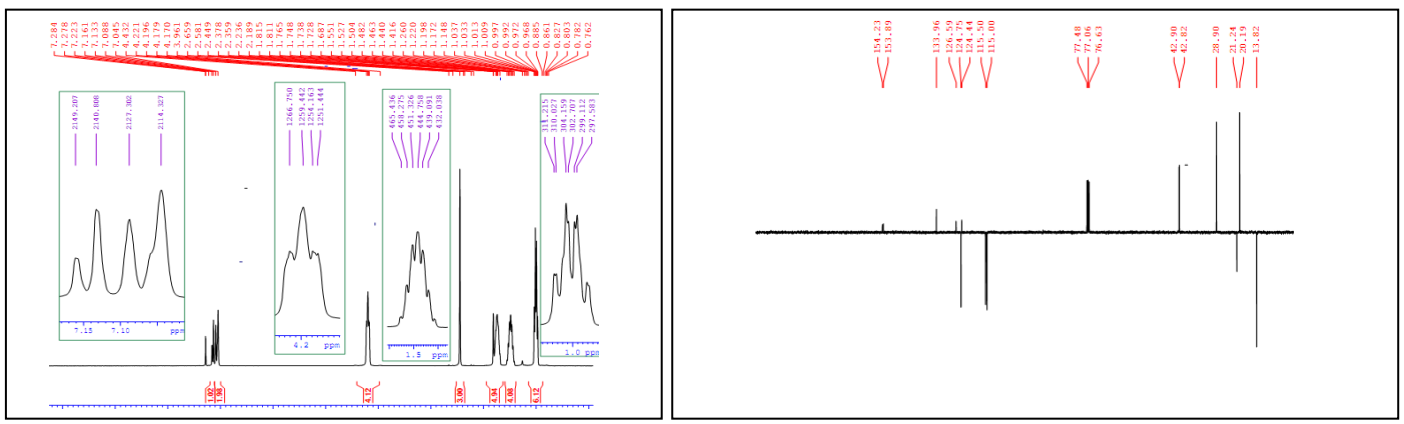

Figure 1: 1H-NMR and 13C-NMR spectrums of 1,4-dibutyl-6-methyl-1,4-dihydroquinoxaline-2,3-dione (AY20).

2.2. Weight loss measurements

Weight loss measurements were carried out in glass vessels containing 100 mL 1 M HCl in the presence and absence of various concentrations of 1,4-dibutyl-6-methylquinoxaline-2,3(1H,4H)-dione (AY20) at 308 K for a 6 h immersion period. Each experiment was performed at least three times to ensure reliability. Average values of the weight loss data were used in corresponding calculations. Inhibition efficiencies (η_w%), were calculated using the relation;

$$\eta_W\ \% = \frac{w_0 - w_i}{w_o} \times 100 \qquad (1)$$

where w_0 and w_i are the values of weight in uninhibited and inhibited solutions, respectively.

3. Results

Many experimental techniques can be used to evaluate the inhibitor efficiencies of inhibitor 1,4-dibutyl-6-methylquinoxaline-2,3(1H,4H)-dione (AY20).

3.1. Weight loss

Weight loss is one of the simplest and best known methods applicable in corrosion studies. Table.1 shows the influence of inhibitor concentration on inhibitor efficiencies (η_w%) after 6 h of immersion at 308 K for each of the inhibitor studied(AY20). Measurements revealed both compound to inhibit corrosion in the acidic media 1M HCl. Corrosion rates were seen to decrease and inhibition efficiencies to increase with increasing additive concentration. At 10^{-3} M, which is the highest concentration applied in the present study, inhibition efficiencies reached values as high as 89 %.

Table1: Corrosion rate and inhibition efficiency in the absence and presence of AY20 in 1.0 M HCl solution.

Inhibitor	*C* (*mol/l*)	C_R (*mg.cm^{-2} h^{-1}*)	*η* (*%*)	*θ*
1M HCl	--	0.82	--	--
Ay20	**10^{-6}**	0.23	72	0.72
	10^{-5}	0.19	77	0.77
	10^{-4}	0.11	87	0.87
	10^{-3}	0.09	89	0.89

3.2. Adsorption isotherm

The necessary information dealing with the interaction between the inhibitor molecules and the mild steel surface are generally provided by adsorption isotherms [19]. The values were tested graphically for fitting a suitable adsorption isotherm. In the present investigation a plotof C_{inh}/θ-C produced straight lines with regression coefficients of 0.99(Fig. 2). Experimental results were in good agreement with the Langmuir adsorption isotherm in accordance with Eq. (x);

$$\frac{C}{\theta} = \frac{1}{K} + C \qquad (2)$$

where C is the inhibitor concentration, θ the fraction of surface coverage and K is the adsorption equilibrium constant. K was obtained from the intercept of the plot and was approximated as 5.8910^5 dm^3mol^{-1}. The standard free energy of adsorption was calculated according to the following equation:

$$\Delta G_{ads} = -RT\ \ln(55.5K) \qquad (3)$$

where R is the universal gas constant, T the thermodynamic temperature that is 308 K in this case and 55.5 is the molar concentration of water in the solution. The Langmuir adsorption isotherm was drawn by plotting C_{inh}/θ versus C_{inh} for various concentrations of inhibitor and considering the θ values from Weight loss studie. The obtained graph was shown in Fig. 2. The straight line obtained in the graph clearly shows that the investigated inhibitor obeys Langmuir adsorption isotherm. Generally, the value of ΔG_{ads} less negative than -20 kJ mol^{-1} signifies physisorption and the value more negative than about -40 kJ mol^{-1} indicates chemisorptions [20]. From this study the calculated $\Delta G_{ads} = -44.22$ kJ/mol values indicates, the process of adsorption is through chemisorption.

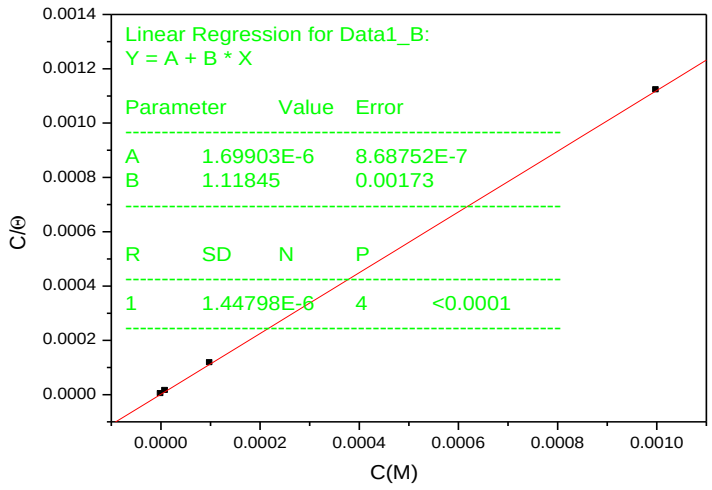

Fig. 2. Langmuir plot (using Weight loss) for mild steel corrosion in 1 M HCl solution with various concentrations of 1,4-dibutyl-6-methylquinoxaline-2,3(1H,4H)-dione (AY20).

3.3. Tafel polarization

Prior to each measurement, attaining a steady state condition on the electrode surface is essential. Following surface pretreatment, the working electrode was immersed in the test solution 1.0 M HCl until the fluctuation in the open circuit potential was under 0.1 mV min^{-1}. The initial E_{ocp} of the blank solution was seen to be −512 mV (vs.SCE), the value becoming constant at approximately −504 mV (vs.SCE) after the first 800 s until the end of the experimental period without much fluctuation. Although 800 s seemed sufficient for the surface to acquire steady state, all experiments were started after 30 min to ensure reliability. Figs. 3 represent the polarization curves of mild steel dissolution in 1.0 M HCl in the absence and presence of various concentrations of the 1,4-dibutyl-6-methylquinoxaline-2,3(1H,4H)-dione (AY20). Table 2, on the other hand, gives some insight into the electrochemical corrosion parameters, i.e., the corrosion potential ($-E_{corr}$), anodic and cathodic Tafel slopes (βa and βc), corrosion current density (i_{corr}) degree of surface coverage (θ) and percentage inhibition efficiency (η_{Pol}%). The addition of 1,4-dibutyl-6-methylquinoxaline-2,3(1H,4H)-dione (AY20) with increasing concentration, gradually decreases the corrosion rate. On the other hand, both the cathodic and anodic current densities show a distinctive decrease leading to a larger decrease in the corrosion current density in the presence of 1,4-dibutyl-6-methylquinoxaline-2,3(1H,4H)-dione (AY20). The slopes of the Tafel lines show small alterations indicating no change in the anodic and cathodic mechanisms leading to the assessment that the inhibitive action of 1,4-dibutyl-6-methylquinoxaline-2,3(1H,4H)-dione (AY20) is due to surface adsorption resulting in the formation of a surface film blocking the active sites [21]. The decrease in the corrosion current density is the highest with respect to the values obtained for 1,4-dibutyl-6-methylquinoxaline-2,3(1H,4H)-dione (AY20).

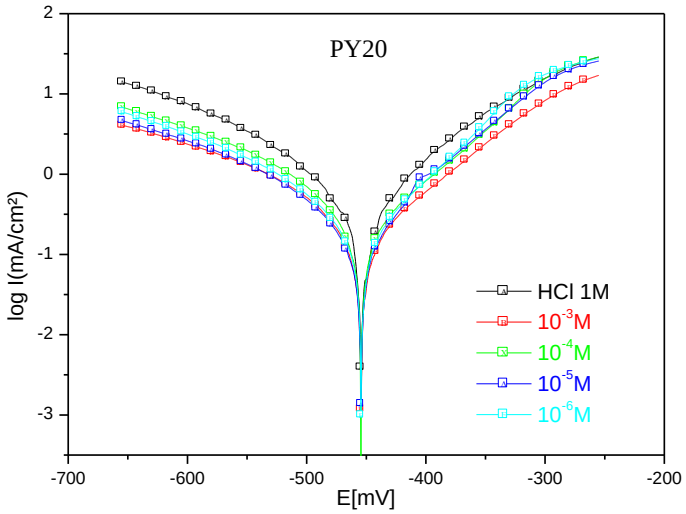

Fig. 3. Potentiodynamic polarization curves for MS in 1 M HCl without and with different concentrations of **AY20** at 308K.

Table 2. Potentiodynamic polarization parameters for the corrosion of MS in 1 M HCl containing different concentrations of PY20 at 308K.

	C (M)	E_{corr} (mV*vs.*CS	I_{corr} (µA/cm^2)	-βc (mV/dec)	βa (mV/dec)	E_p (%)
HCl	Blank	-450	1381	140	185	--
PY2	10^{-3}	-455	395	119	117	71
	10^{-4}	-454	247	124	120	82
	10^{-5}	-455	188	131	105	86
	10^{-6}	-457	139	111	94	90

3.4. Impedance (EIS) studies

The EIS studies were investigated by varying the concentrations of 1,4-dibutyl-6 methylquinoxaline-2,3(1H,4H)-dione (AY20) in 1.0 M HCl at temperature 308k. From this study, the impedance diagrams were obtained and are shown in Fig. 4. The impedance data such as R_{ct}, C_{dl} and θ were obtained from Nyquist plot. The impedance function of the CPE has the form [22].

$$Z_{CPE} = \frac{1}{Y_0(j\omega)^n} \quad (4)$$

WhereY_0 is a proportionality coefficient, j is the imaginary number, ω is the angular frequency ($\omega=2\pi f$, here f is the AC frequency in Hz), and n is a phase shift, which is related to the system homogeneity. When the CPE represents a pure capacitor, n=1. The capacitance values (C_{dl}) can be calculated as follow:

$$C_{dl} = \frac{Y_0\omega^{n-1}}{\sin(n\pi/2)} \quad (5)$$

The percentage of inhibition efficiency is determined from R_{ct} values according to the above-mentioned equation and all the impedance parameters are given in Table 3. The impedance studies clearly indicate that the Rct value increased and C_{dl} values decreased with the addition of 1,4-dibutyl-6 methylquinoxaline-2,3(1H,4H)-dione (AY20) concentration. The increasing Rct values imply reduced corrosion rate in the presence of the studied inhibitor and this is because of the increasing surface coverage of 1,4-dibutyl-6 methylquinoxaline-2,3(1H,4H)-dione (AY20) molecule on the addition and resulting in the formation of protective film on the corroded mild steel surface [23, 24]. The decrease in C_{dl} values was due to the gradual replacement of water molecules by the adsorption of 1,4-dibutyl-6 methylquinoxaline-2,3(1H,4H)-dione (AY20) compound at MS/solution interface, which led to the formation of protective film on the corroded mild steel surface and also prevent the further form of corrosion products [25]. From Figs. 5,4 the phase angle increases with increase in the investigated inhibitor concentration this is due to the adsorption of inhibitor molecule on the surface of mild steel [26]. According to the appearance of the phase angles versus frequency diagrams, the increasing concentration of the studied inhibitor 1,4-dibutyl-6 methylquinoxaline-2,3(1H,4H)-dione (AY20) in the presence of acidic chloride solution results in more negative values of the phase angle at high frequencies, indicating superior inhibitive behavior at higher concentrations. This result could be attributed to higher corrosion activity even at low concentrations of 1,4-dibutyl-6 methylquinoxaline-2,3(1H,4H)-dione (AY20) [27]. The obtained inhibition efficiency by this study showed good agreement with the result obtained from weight loss study.

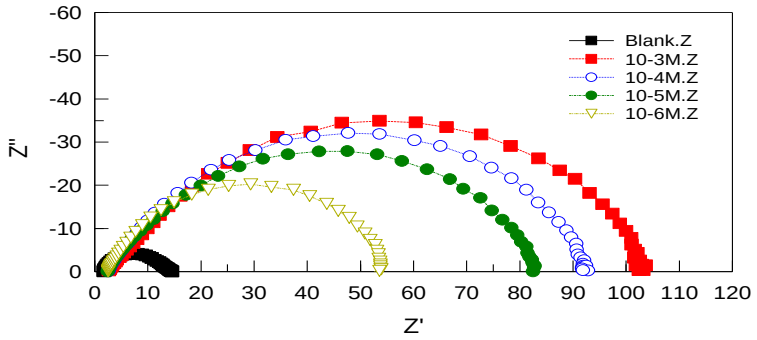

Fig. 4. Nyquist plots for mild steel corrosion in 1 M HCl solution with various concentrations of **AY20**.

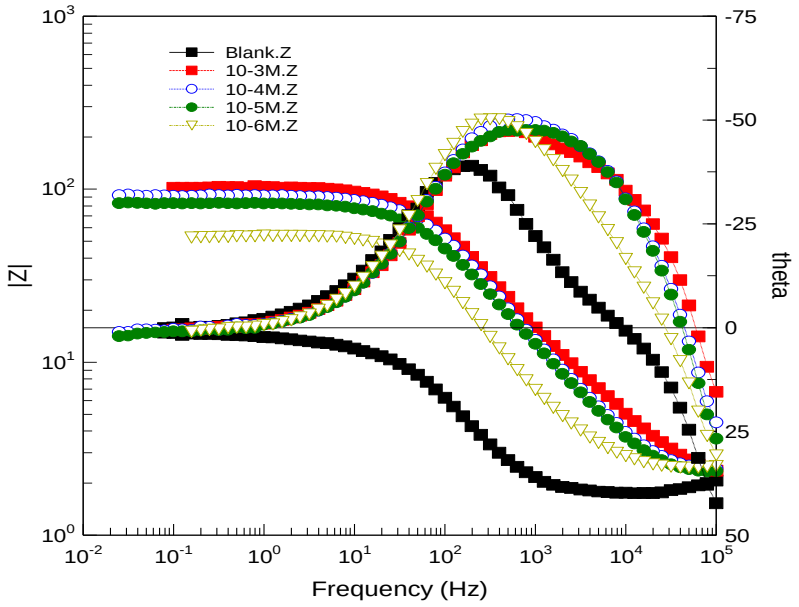

Fig. 5. Bode plots for mild steel corrosion in 1 M HCl solution with various concentrations of **AY20**.

Table 3. Corrosion parameters obtained from EIS studies of mild steel in 1 M HCl Solution containing different concentrations of **AY20**.

Concentration (M) / Prameters	**1M HCl**	**10^{-6}**	**10^{-5}**	**10^{-4}**	**10^{-3}**
Real Center	9.25	28.36	43.01	47.80	53.50
Imag. Center	1.62	6.00	15.14	15.45	18.49
Diameter	15.13	52.46	85.79	94.75	106.33
N	0.81	0.83	0.84	0.83	0.91
Low Intercept R_s ($\Omega.cm^2$)	1.86	2.8314	2.8767	3.014	3.6585
High Intercept R_t ($\Omega.cm^2$)	16.64	53.899	83.145	92.588	103.35
Depression Angle	12.42	13.23	20.67	19.03	20.35
ω_{max} (rad s^{-1})	929.60	419.96	482.34	497.24	500.75
Estimated R_t($\Omega.cm^2$)	14.78	51.06	80.26	89.57	99.68
Estimated C_{dl}($F.cm^{-2}$)	7.11E-5	4.53E-5	2.41E-5	2.12E-5	1.87E-5
E (%)	--	77	85	87	89

The corrosion behavior of MS in 1.0 M HCl solution was also studied in the presence and absence of 1,4-dibutyl-6-methylquinoxaline-2,3(1H,4H)-dione (AY20) using the EIS technique. Nyquist plots are shown in Fig.4 . It is clear from both plots that the impedance response of MS in the 1.0 M HCl is significantly effected after the addition of 1,4-dibutyl-6-methylquinoxaline-2,3(1H,4H)-dione (AY20). Both spectrums show only one depressed capacitive semi-circle where the low frequency intersection is related to the resistance against electron transfer. Similar results have been reported for mild steel in acidic media by various researchers [28–29]. The standard Randles' circuit model, represented in Fig. 6, can be applied to determine the solution resistance (R_s), transfert resistance (R_{ct}) and constant phase element (CPE) as pointed out in a recent study [30]. The so called "dispersing effect", as a result of surface roughness, surface inhomogeneity and the adsorption phenomena is said to lead to the formation of depressed semi-circles which are under the real axis [31–32]. Deformation is said to be the result of geometrical factors due to this dispersing effect [33, 34]. In order to compensate for the non ideal capacitive behavior at the metal/solution interface, a constant phase element (CPE) was introduced into the equivalent circuit (Fig.6). Taking into consideration the relation between the transfert resistance (Rct) and the double layer capacitance (Cdl) given in literature [35], Cdl values have been calculated and represented in Table 3 alongside the fitted results. The Bode and phase angle plots for mild steel in 1.0 M HCl with and without 1,4-dibutyl-6 methylquinoxaline-2,3(1H,4H)-dione (AY20) is given in Figs. 4,5. The increase of the absolute impedance at low frequencies in the Bode plots, confirms the higher degree of protection with increasing additive concentration. A single phase peak between 0 to 50° reveals the presence of a one time constant in the presence of 1,4-dibutyl-6 methylquinoxaline-2,3(1H,4H)-dione (AY20) due to the formation of an electrical double layer at the solution-surface interface [36, 37]. The dependence of inhibition efficiencies on a time scale have also evaluated up to 1/2 h, with the EIS method for a concentration of 10^{-3} M at 308K. Measurements were recorded after the initial 30 min in order to guarantee steady state at the beginning. Inhibition efficiencies were graphed against time as seen in Fig. 7.

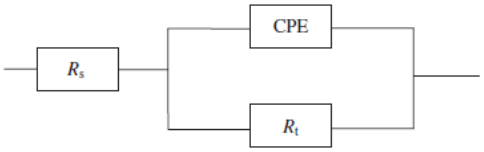

Fig. 6. Equivalent circuit used to fit the EIS data.

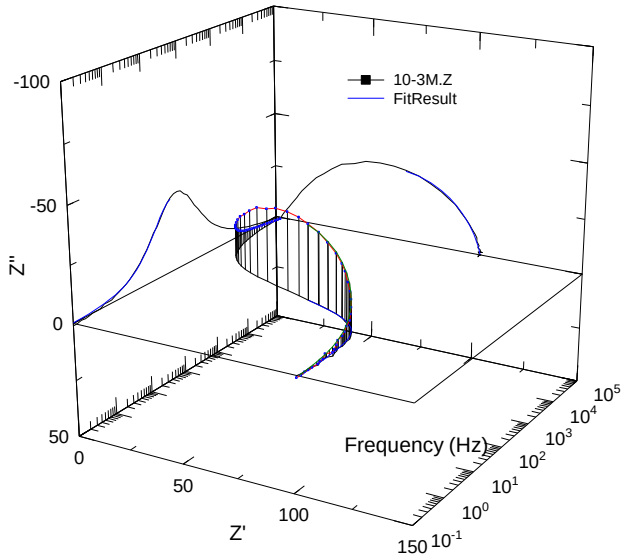

Fig. 7. EIS Nyquist and Bode diagrams 3D for mild steel/1 M HCl + 10^{-3} M of AY20 interface: (------) experimental; (------) fitted data.

3.5. Theoretical study

3.5.1. Quantum chemical calculations

In the last few years, the FMOs (HOMO and LUMO) are widely used for describing chemical reactivity. The HOMO containing electrons, represents the ability (E_{HOMO}) to donate an electron, whereas, LUMO haven't not electrons, as an electron acceptor represents the ability (E_{LUMO}) to obtain an electron. The energy gap between HOMO and LUMO determines the kinetic stability, chemical reactivity, optical polarizability and chemical hardness–softness of a compound [38]. In this paper, we calculated the HOMO and LUMO orbital energies by using B3LYP method with 6-31G(d,p). All other calculations were performed using the results with some assumptions. The higher values of E_{HOMO} indicate an increase for the electron donor and this means a better inhibitory activity with increasing adsorption of the inhibitor on a metal surface, whereas E_{LUMO} indicates the ability to accept electron of the molecule. The adsorption ability of the inhibitor to the metal surface increases with increasing of E_{HOMO} and decreasing of E_{LUMO}. High ionization energy (I= 6.67 eV, I= 3.46 eV in gas and aqueous phases respectively) indicates high stability [39-41], the number of electrons transferred (ΔN) was also calculated and tabulated in Table 4. The number of electrons transferred (ΔN) was also calculated and tabulated in Table 5. The ΔN(gas) < 3.6 and ΔN(aqueous) < 3.6 indicates the tendency of a molecule to donate electrons to the metal surface [42, 43].

Table 4. Quantum chemical descriptors of the studied inhibitor at B3LYP/6-31G(d,p) in gas, G and aqueous, A phases

	Phase	
Prameters	**Gas**	**Aqueous**
Total Energy *TE* (eV)	-25087.8	-25088.3
E_{HOMO} (eV)	-6.6719	-5.9089
E_{LUMO} (eV)	-0.5181	-1.6620
Gap ΔE (eV)	6.1538	4.2469
Dipole moment μ (Debye)	6.8737	10.0659
Ionisation potential I (eV)	6.6719	5.9089
Electron affinity A	0.5181	1.6620
Electronegativity χ	3.5950	3.7855
Hardness η	3.0769	2.1235
Electrophilicity index ω	2.1001	3.3741
Softness σ	0.3250	0.4709
Fractions of electron transferred ΔN	0.5533	0.7569

The final optimized geometries of 1,4-dibutyl-6 methylquinoxaline-2,3(1H,4H)-dione (AY20) in gas and aqueous, selected valence bond angle and dihedral angles and bond lengths are given in Figure8.

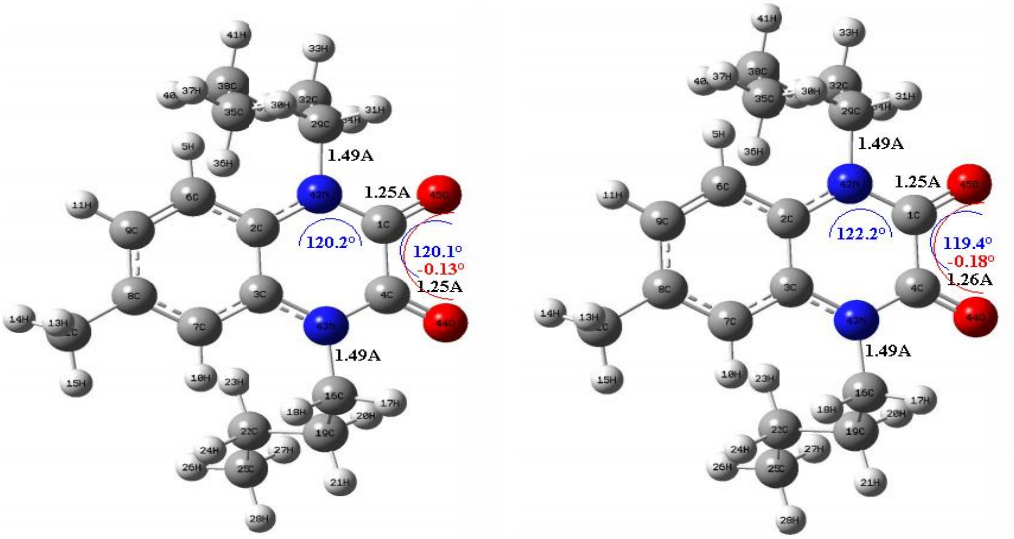

AY20 Gas phase **AY20** Aqueous phase

Figure 8. Optimized molecular structures, selected dihedral angles (red), valence bond angle (blue) and bond lengths (black) of the studied inhibitors calculated in gas and aqueous phases at B3LYP/6-31G(d,p) level of (AY20).

After the analysis of the theoretical results obtained, we can say that the molecule 1,4-dibutyl-6 methylquinoxaline-2,3(1H,4H)-dione (AY20)have a non-planar structure.

Table 6 : The HOMO and the LUMO electrons density distributions of the studied inhibitors computed at B3LYP/6-31G (d,p) level in gas and aqueous phases.

	AY20 Gas phase	**AY20** Aqueous phase
HOMO	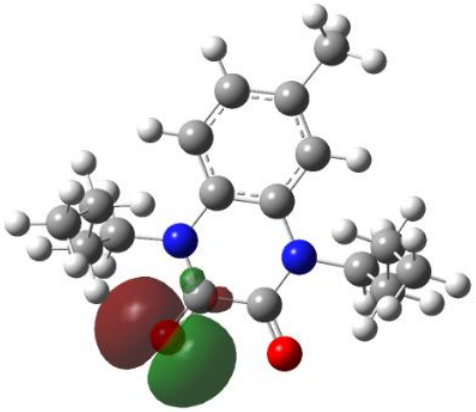	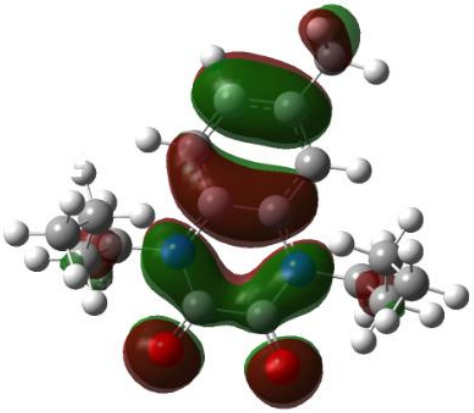
LUMO	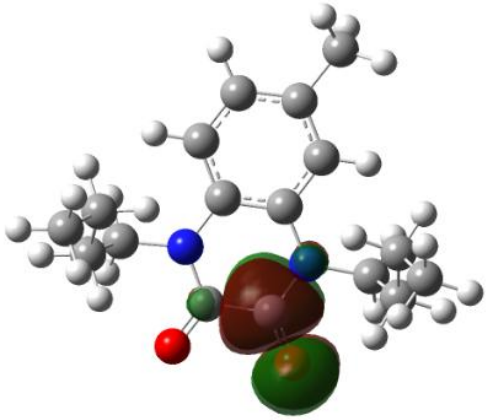	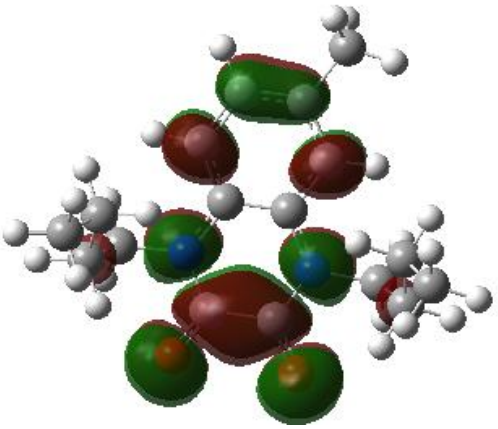

The inhibition efficiency afforded by the 1,4-dibutyl-6 methylquinoxaline-2,3(1H,4H)-dione (AY20) may be attributed to the presence of electron rich O.

4. Conclusion

From the overall experimental results the following conclusions can be deduced:

- 1,4-dibutyl-6 methylquinoxaline-2,3(1H,4H)-dione (AY20) act as good mild steel corrosion inhibitors in 1M HCl. All electrochemical tests are in good agreement with the maximum percentage of inhibition efficiency obtained at the concentration of 10^{-3} M of AY20.
- Potentiodynamic polarization measurements demonstrate that 1,4-dibutyl-6 methylquinoxaline-2,3(1H,4H)-dione (AY20) act as mixed-type inhibitor.
- Thermodynamic investigations confirmed that the adsorption of organic molecule on the mild steel surface obeys The Langmuir adsorption isotherm.
- The negative values of free energy of adsorption indicate that the adsorption process is spontaneous on the mild steel surface.
- The standard Randles' circuit model has been applied as the equivalent circuit compatible with the experimental impedance data.
- Theoretical results confirm the experimental data.

References

[1] H. Elmsellem, T. Harit, A. Aouniti, F. Malek, A. Riahi, A. Chetouani, B. Hammouti, Protection of Metals and Physical Chemistry of Surfaces. 51 (2015) 873–884.

[2] H. Elmsellem , H.Nacer, F.Halaimia, A.Aouniti, I.Lakehal, A.Chetouani, ,Int. J. Electrochem. Sci, 9 (2014) 5328-5351.

[3] Z.Tribak, Y.Kandri Rodi, H. Elmsellem, I. Abdel-Rahman, A. Haoudi, M. K. Skalli, J. Mater. Environ. Sci. 8 (2017) 1116 -1127.

[4] H. Elmsellem, N. Basbas, A. Chetouani, A. Aouniti, Portugaliae. Electrochimica Acta, 2 (2014) 77-108.

[5] H. Elmsellem, K. Karrouchi, Der PharmaChemica, 7 (2015) 237-245.

[6] H. Elmsellem , M. H. Youssouf, A. Aouniti, Russian, Journal of Applied Chemistry. 8 (2014) 744−753.

[7] H. Darmokoesoemo, H.Setyawati, A. T .A. Ningtyas,Y. Kadmi, Heri Septya Kusuma. Results in Physics. http://dx.doi.org/10.1016/j.rinp.2017.08.009

[8] H. Elmsellem, A. Aouniti, Youssoufi, H. Bendaha,T. Ben hadda, A. Chetouani , Warad I., Hammouti B., Phys. Chem. News, 70 (2013) 84.

[9] H. Elmsellem, Elyoussfi A., Sebbar N. K., Dafali A., Cherrak K., Steli H., Essassi E. M., Aouniti A. and Hammouti B., Maghr. J. Pure & Appl. Sci, 1 (2015) 1-10.

[10] H. Elmsellem, Aouniti A.,Khoutoul M., Chetouani A., Hammouti B., Benchat N., Touzani R. and Elazzouzi M., J. Chem. Pharm. Res, 6 (2014) 1216.

[11] G. Aridoss, S. Balasubramanian, P. Parthiban, and S. Kabilan, Eur. J Med. Chem. 41 (2006) 268–275.

[12] V. Bavetsias, C. Sun, N. Bouloc, J. Reynisson, P. Workman,S. Linardopoulos and E. McDonald, Bioorg. Med. Chem. Lett. 17 (2007) 6567–6571.

[13] A. Dell, D. H. William, H. R. Morris, G. A. Smith, J. Freeney and G. C. K. Roberts, 97(1975) J.Am. Chem. Soc. 2497.

[14] C. Bailly, S. Echepare, F. Gago and M. J. Waring, Anticancer 15 (1999) Drug Des. Chem. 270.

[15] R.H. Bahekar, M.R. Jain, A. A. Gupta, A. Goel, P.A. Jadav, D.N. Patel, V.M. Prajapati, and Patel, P.R., 340 (2007) Arch. Pharm. (Weinhein), 359-366.

[16] H.M. Refaat, A.A. Moneer, and O.M. Khalil, 27 (2004) Arcll. Pharm.Res. 1093-1098.

[17] S.A.M. EI-Hawash, and A. E. Abdei-Wahab, 339 (2006)Arch. Pharm. (Weinhein), 437-447.

[18] M. Loriga, S. Piras, P. Sanna and G. Parlietti, 52 (1997) Farmaco. 157-166.

[19] M. Sikine, H. Elmsellem, Y. Kandri Rodi, H. Steli, A. Aouniti, B. Hammouti, Y. Ouzidan, F. Ouazzani Chahdi, M. Bourass, and E. M. Essassi, J. Mater. Environ. Sci. 7 (2016) 4620-4632.

[20] S. Bourichi, Y. Kandri Rodi, H. Elmsellem, H. Steli, Y. Ouzidan, N. K. Sebbar, F. Ouazzani Chahdi, E. M. Essassi, F. El-Hajjaji and B. Hammouti, Der Pharma Chemica, 8 (2016) 179-186.

[21] H. Elmsellem, Elyoussfi A., Steli H., Sebbar N. K., Essassi E. M., Dahmani M., El Ouadi Y., Aouniti A., El Mahi B., Hammouti B., Der Pharma Chemica,8 (2016) 248-256.

[22] L. Pauling, The nature of the chemical bond, 3rd edn. Cornell University Press, Ithaca, 1960.

[23] K.D. Sen and C. Jorgenson, Structure and bonding: electronegativity, Springer, Berlin, 1987, 66.

[24] H. Bendaha, H. Elmsellem, A. Aouniti, M. Mimouni, A.Chetouani, B. Hammouti, Physicochemical Mechanics of Materials. 1 (2016) 111-118.

[25] Y. Filali Baba, H. Elmsellem, Y. Kandri Rodi, H. Steli , Y. Ouzidan , F. Ouazzani Chahdi, Der Pharma Chemica. 8 (2016)159-169.

[26] P. Geerlings, F. de Proft and W. Langenaeker, Chem. Rev., 103 (2003) 1793-1873.

[27] Z.Tribak, Y. Kandri Rodi, H. Elmsellem, J. Mater. Environ. Sci. 8 (2017) 1116 -1127.
[28] R.G. Parr, R.A. Donnelly, M. Levy and W. Palke, J. Chem. Phys., 68 (1978) 3801-3807.
[29] P. Hohenberg, Kohn, Phys. Rev. B., 136 (1964) 864-871.
[30] W. Kohn and L. Sham, J. Phys. Rev. A., 140 (1965) 1133.
[31] M. Ramdani, H. Elmsellem, N. Elkhiati, B.Haloui, A. Chetouani and B. Hammouti , Der Pharma Chem.7 (2015) 67-76.
[32] R.Chadli, Elazouzi M., Khelladi I., Elhourri A.M., H. Elmsellem, Aouniti A., Kajima Mulengi J., Hammouti B., Portugaliae Electrochimica Acta. 35 (2017) 65-80.
[33] M. Y.Hjouji, M.Djedid, H. Elmsellem, Kandri Rodi Y., Benalia M., Steli H., Ouzidan Y., Ouazzani Chahdi F., Essassi E. M., Hammouti B., Der Pharma Chemica. 8 (2016) 85-95.
[34] S.Lahmidi, H. Elmsellem, A. Elyoussfi, N. K. Sebbar, Y. Ouzidan, Y. KandriRodi , and B. Hammouti, Der Pharma Chemica. 8 (2016) 294-303.
[35] G. Aziate, H. Elmsellem, N.K. Sebbar, Y. El Ouadi, J. Mater. Environ. Sci, 8 (2017) 3873-3883.
[36] A. Elyoussfi, A. Dafali, H. Elmsellem, H. Steli, Y. Bouzian Y, J. Mater. Environ. Sci. 7 (2016) 3344-3352.
[37] I. Chakib, H. Elmsellem, Sebbar N. K., Lahmidi S., Nadeem A., Essassi E. M., Ouzidan Y., Abdel-Rahman I., Bentiss F., B. Hammouti., J. Mater. Environ. Sci, 7 (2016) 1866-1881.